# Fluorination Effects on the Structural Stability and Electronic Properties of sp^3-type Silicon Nanotubes

Alon Hever, Jonathan Bernstein, and Oded Hod*

Department of Chemical Physics, School of Chemistry, The Raymond and Beverly Sackler Faculty of Exact Sciences, Tel-Aviv University, Tel-Aviv 69978, Israel

Ⓢ *Supporting Information*

ABSTRACT: A density functional theory study of the structural and electronic properties and relative stability of fluorinated sp^3 silicon nanotubes and their corresponding silicon nanowires built along various crystallographic orientations is presented. The structural stability is found to increase linearly with fluorine surface coverage, and for coverages exceeding 25%, the tubular structures are predicted to be more stable than their wirelike counterparts. The band gaps of the fully fluorinated systems are lower than those of their fully hydrogenated counterparts by up to 0.79 eV for systems having a relatively low silicon molar fraction. As the silicon molar fraction increases, these differences appear to reduce. For mixed fluorination and hydrogenation surface decoration schemes, the band gaps usually lie between the values of the fully hydrogenated and fully fluorinated systems. Furthermore, the band gap values of the silicon nanotubes are found to be more sensitive to the fluorine surface coverage than those of the silicon nanowires. These results indicate that surface functionalization may be used to control the stability of narrow quasi-one-dimensional silicon nanostructures and opens the way toward chemical tailoring of their electronic properties.
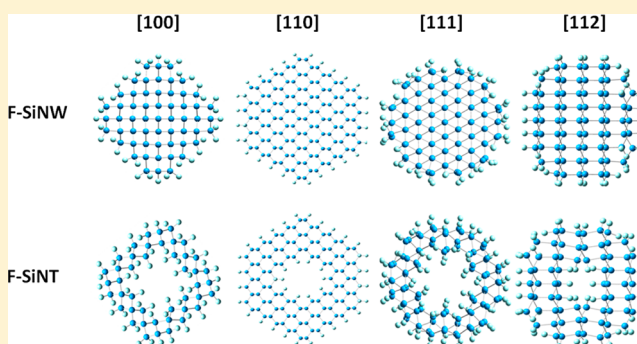
INTRODUCTION

Due to their unique and diverse physical properties, quasi-one-dimensional silicon nanostructures show great promise to serve as active components in various nanoscale devices including sensitive chemical and biological detectors,[1-7] electronic components such as nanoscale field-effect transistors,[8,9] optoelectronic devices,[10-12] solar cells,[13-16] and water-splitting photocatalysts.[17] Since different applications require different electronic properties, it is desirable to identify efficient and accessible routes to control and tailor the electronic structure of such systems. To this end, experimental and theoretical studies of silicon nanowires (SiNWs) have revealed several factors that may influence the size and character of their band gap. These include the diameter of the SiNW,[18-26] its growth orientation,[20,23,26,27] cross-sectional shape,[28,29] surface reconstruction,[26] chemical passivation[27,30-33] and doping,[34] and strain effects.[35-37]

To gain control over the geometrical parameters of SiNWs, several fabrication methods have been developed, including laser ablation and electron beam evaporation metal-catalytic vapor—liquid—solid methods[32,38-42] and oxide-assisted catalyst-free approaches,[43-45] as well as solution-based techniques.[46] These methods yield wires with different crystallographic orientations and dimensions scaling down to diameters that are in the single-nanometer regime.[32,38,43,47] The effects of chemical modifications on the physical properties of SiNWs have been investigated experimentally in several recent studies,

as well. Here, it was shown that hydrogen-passivated SiNWs can be achieved via removal of the oxide layer often decorating their surface.[39,43,47-55] Alternatively, surface hydrogenation can be achieved by using hydrogen as a carrier gas in the chemical vapor deposition process.[42]

From the theoretical perspective, hydrogen passivation of SiNWs is attractive in terms of lowering the computational burden. Hence, many of the earlier theoretical studies of SiNWs have adopted hydrogen passivated SiNW models.[20,24,26,56,57] These were followed by several recent studies using hydrogenated SiNW models as reference systems for SiNWs with other chemical passivation schemes.[27,30,31,58-60] It was shown that decoration with hydroxyl and amine groups tends to cause diameter-dependent band gap red shifts with respect to the hydrogen-passivated systems.[27,30]

The effects of surface halogenation of [110] SiNWs with diameters varying from 0.6 to 3 nm were studied by Leu et al.,[31] who showed that increased halogen surface coverage tends to decrease the band gap of the SiNW. As may be expected, larger band gap variations were found for narrower wires, which have a larger surface to volume ratio. Furthermore, the identity of the halogen atom was found to impact the resulting band gap of the system, where larger halogen atoms resulted in more

pronounced effect on the band gap. Bondi et al.[53] have shown that for SiNWs grown along the [111] orientation, fluorine surface decoration results in increased band density. Studying the effects of crystallographic orientation, Ng et al.[61] have reported band gap decrease of up to 1 eV with increasing [100], [110], [111], and [112] SiNW surface coverage of fluorine and hydroxyl groups. For the fluorinated SiNWs, the conduction band minimum (CBM) and valence band maximum (VBM) energies were found to strongly decrease with respect to the fully hydrogenated counterparts.

Going beyond SiNW structures, we have recently presented a computational study exploring the structural and electronic properties of fully hydrogenated sp^3-type silicon nanotubes (SiNTs) grown along various crystallographic directions.[71] Here, all SiNTs studied were found to be less (meta-)stable than the corresponding SiNWs while possessing an increased band gap. In light of the recent intensive work on chemical decoration of SiNWs, it would be interesting to explore the effects of surface functionalization on the structural stability and electronic properties of SiNTs. In the present work, we address this issue, showing that surface fluorination is expected to dramatically increase the relative stability of quasi-one-dimensional silicon structures as compared to their hydrogenated counterparts. Furthermore, we show that surface chemistry may be used as a simple means to control the electronic properties of SiNWs and SiNTs.

To this end, we reconsider the eight SiNWs and SiNTs models studied in ref 71 with growth orientations along the [100], [110], [111], and [112] silicon crystal directions (see 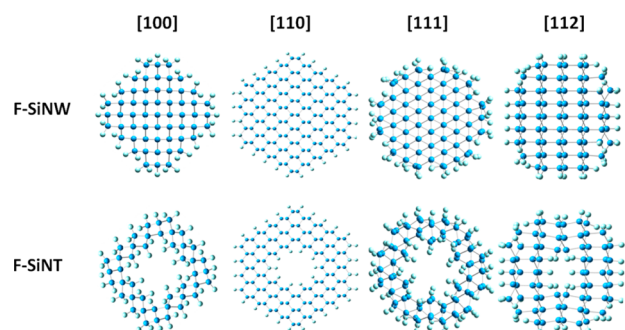Figure 1). Using the hydrogenated systems as reference, we then partially or fully substitute passivating hydrogen atoms with fluorine atoms. For the partial substitution schemes, we consider fluorine surface coverage of 25%, 50%, and 75% where the substitution sites are determined randomly, and for each coverage three different random substitution schemes are considered. We note that the experimental realization of narrow SiNTs has been recently achieved,[72−78] showing the ability to control their surface chemistry.[76,77]

All calculations have been performed by density functional theory (DFT) as implemented in the Gaussian09 suite of programs.[79] Three different functional approximations have been considered: namely, the local density approximation (LDA),[80,81] the Perdew−Burke−Ernzerhof (PBE) realization of the generalized gradient approximation,[82] and the screened exchange hybrid density functional of Heyd, Scuseria, and Ernzerhof (HSE).[83−85] The latter functional has been tested for a wide set of materials and was shown to accurately reproduce experimental structural parameters and band gaps.[71,86,87] Initial geometry optimizations have been performed using the LDA with the 3-21G atomic centered Gaussian basis set. Further geometry relaxation, including lattice vectors and atomic positions optimization, has been performed for each functional approximation separately by use of the double-ζ polarized 6-31G** basis set.[88] The relaxed radial dimensions of the different SiNTs and SiNWs are summarized in Table 1. Coordinates of the fully relaxed structures can be found in the Supporting Information.

STABILITY

We start by analyzing the relative structural stability of the different NWs and NTs shown in Figure 1. As the SiNW and SiNT structures have different chemical compositions, the cohesive energy per atom does not provide a suitable measure for comparison of their relative stability. Therefore, we define the Gibbs free energy of formation (δG) for a SiNT and a SiNW as[26,27,71,89]

$$\delta G(\chi_i) = E(\chi_i) - \sum_i \chi_i \mu_i \tag{1}$$

where $E(\chi_i)$ (i = Si, H, F) is the cohesive energy per atom of a SiNW/NT of a given composition, χ_i is the molar fraction of atom i in the system with $\sum_i \chi_i = 1$, and μ_i is the chemical potential of element i. Here, we choose μ_H and μ_F as the binding energy per atom of the ground state of the H_2 and F_2 molecules, respectively, and μ_{Si} as the cohesive energy per atom of bulk silicon. This definition allows for a direct energetic comparison between SiNW/NTs with different chemical compositions, where negative values represent stable structures with respect to the constituents. It should be stressed that this

Figure 1. Schematic representation of various fluorinated SiNWs and SiNTs carved out of bulk silicon along the [100], [110], [111], and [112] crystallographic orientations. Light blue and gray spheres represent silicon and fluorine atoms, respectively.

Table 1. Average Radial Dimensions of Fully Fluorinated Silicon Nanotube and Nanowire Structures[a]

| | diameter (nm) | | | | | | | | |
| | SiNW | | | SiNT, outer | | | SiNT, inner | | |
	LDA	PBE	HSE	LDA	PBE	HSE	LDA	PBE	HSE
[100]	1.76	1.78	1.77	1.80	1.83	1.82	0.65	0.70	0.69
[110]	2.63	2.66	2.65	2.61	2.65	2.64	1.36	1.38	1.38
[111]	1.77	1.80	1.79	1.81	1.86	1.84	0.89	0.92	0.91
[112]	1.81	1.84	1.82	1.79	1.84	1.83	0.45	0.46	0.45

[a]Structures were optimized by use of the LDA, PBE, and HSE exchange−correlation functional approximations and the 6-31G** basis set. The [110] dimensions have been obtained by use of only the 3-21G basis set due to the computational burden. Reported diameters are twice the average radius from the axis of the SiNW/SiNT to the external layer of silicon atoms.

treatment gives a qualitative measure of the relative stability while neglecting thermal and substrate effects and zero-point energy corrections.[27]

In Figure 2 we plot δG as calculated from eq 1 for the fully fluorinated SiNWs and SiNTs considered. For comparison, we
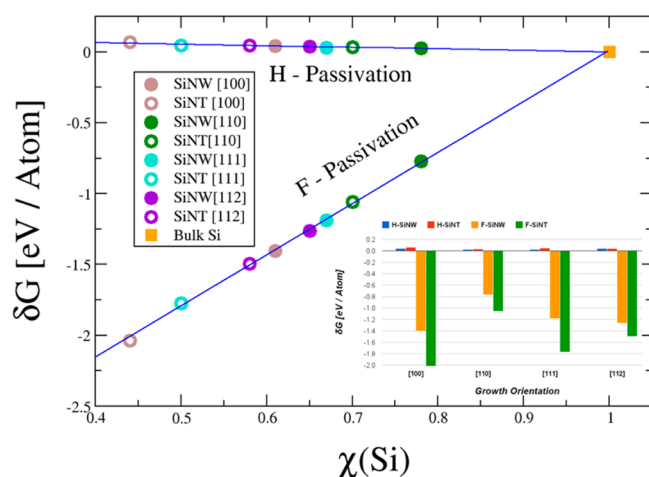

Figure 2. δG as calculated from eq 1 at the HSE/6-31G** level of theory for the different fully hydrogenated and fully fluorinated SiNWs and SiNTs considered. (Inset) Comparison of δG values between fully hydrogenated and fully fluorinated SiNW and SiNT models with similar growth orientation. To reduce the computational burden, geometry optimization of the fluorinated [110] SiNW and SiNT has been performed at the LDA/3-21G and HSE/3-21G level of theory, respectively. Single-point calculations performed at the HSE/6-31G** level of theory with the obtained geometries of both structures were used to evaluate δG. We estimate that this procedure introduces errors of less than 40% in the calculated values (see Supporting Information).

include the results obtained in ref 71 for the fully hydrogenated systems. Similar to the case of the latter, we identify a linear relationship between the molar fraction of silicon atoms and the relative stability of the fully fluorinated SiNWs/SiNTs considered. Nevertheless, while the stability of the various hydrogenated systems was found to decrease with decreasing silicon molar fraction, the fluorinated structures present a completely opposite picture both qualitatively and quantitatively. When the hydrogenated structures are compared to their fluorinated counterparts, a considerable increase in stability is obtained upon fluorine decoration. The stability is further enhanced as the molar fraction of silicon content decreases. Furthermore, unlike the case of the hydrogen-passivated structures, it is found that the fluorinated SiNTs considered are more stable than their SiNW counterparts (see inset of Figure 2).

These observations can be rationalized by considering the dissociation energies of the Si−F, Si−H, and Si−Si bonds, which were measured to be ~160, ~90 [in (fluoro)silanes], and 54 kcal/mol (in bulk form), respectively.[90] As can be seen, the Si−F bond is about 1.8 times stronger than the Si−H bond. In fact, the Si−F bond is among the strongest single bonds known, thus explaining the increased stability upon replacement of surface hydrogens with fluorine atoms. Furthermore, since we are considering relatively narrow NTs, the destabilization effect of the extraction of the inner silicon core of the wire is found to be fully compensated by the Si−F bonds formation on the NT's inner surface, thus resulting in systems that are even more stable than the corresponding NWs. This is in contrast to the

case of the hydrogenated systems where, due to the weaker nature of the Si−H bond, even for the narrowest system considered the absence of the inner silicon core is not energetically compensated by the hydrogenation of the NT's inner surface and the wire structures are found to be more stable than the corresponding tubes.

Next, we examine the relative stability of the [100] and [112] SiNWs and SiNTs with mixed hydrogenation and fluorination decoration schemes. Figure 3 (lower panels) shows the
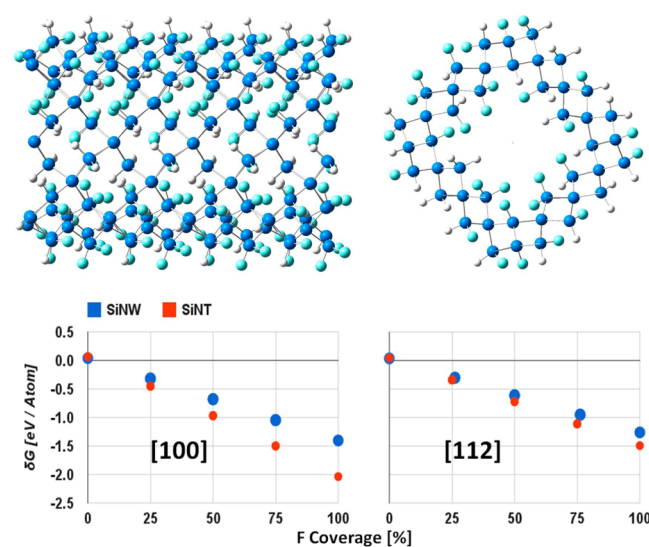

Figure 3. Relative stability of SiNWs and SiNTs with mixed hydrogen and fluorine surface decoration schemes. The upper panels provide side (upper left) and axial (upper right) views of the [100] SiNT with 50% fluorine surface coverage. The lower panels present δG as calculated from eq 1, at the HSE/6-31G** level of theory, for the [100] (lower left) and [112] (lower right) SiNWs and SiNTs with varying fluorine and hydrogen coverage. For the [112] SiNT with 50% fluorine coverage, only two (instead of three) random decoration schemes have been calculated. Results of all random configurations considered for the mixed structures are presented.

calculated δG values for these systems as a function of fluorine surface coverage, where 0% represents the fully hydrogenated systems and 100% stands for the fully fluorinated systems. As may be expected from the analysis presented above, the stability increases with increasing fluorine coverage. Interestingly, already at ~25% fluorine coverage the SiNT structures become more stable than their corresponding SiNWs. Unless otherwise mentioned, for each partial fluorine coverage studied, three random decoration schemes were considered. An example of the [100] SiNT with one of the 50% fluorine surface coverage schemes is presented in the upper panels of Figure 3. We find that differences between the relative stabilities of the various decoration schemes at a given fluorine surface coverage are on the order of 0.01 eV/atom and are thus too small to be noticed in the diagrams presented in the lower panels of Figure 3.

■ ELECTRONIC PROPERTIES

We now turn to study the electronic properties of the various systems considered. We start by analyzing the effects of crystallographic orientation and surface passivation scheme on the band gap of the SiNWs and their corresponding SiNTs studied. Figure 4 presents a detailed description of these results where the band gap is plotted against the molar fraction of
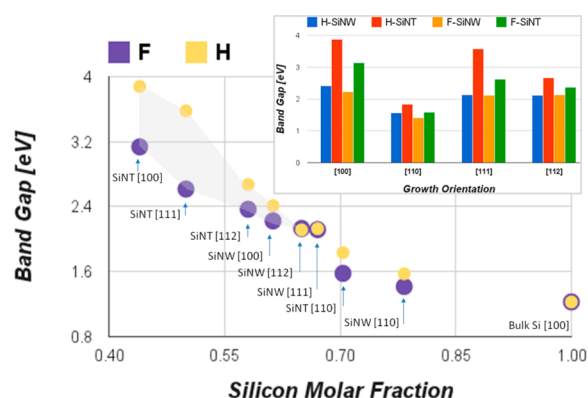
Figure 4. Band gap vs silicon molar fraction for the fluorinated SiNWs and SiNTs studied (purple circles). Results for the fully hydrogenated system are taken from ref 71 and are presented for comparison purposes (orange circles). The transparent gray area indicates the region spanned between the band gap values of the fully hydrogenated and fully fluorinated systems. Inset: Comparison between band gaps of fully hydrogenated and fluorinated SiNWs and SiNTs at different growth orientations. To reduce computational burden, geometry optimization of the fluorinated [110] SiNW and SiNT has been performed at the LDA/3-21G and HSE/3-21G level of theory, respectively. Single-point calculations performed at the HSE/6-31G** level of theory using the obtained geometries of both structures were used to evaluate the band gaps. We estimate that this procedure introduces errors of less than 8% in the calculated values (see Supporting Information).

silicon atoms within each system. As can be seen, similar to the case of the fully hydrogenated systems[71] (light orange circles), the band gap of the fully fluorinated SiNWs and SiNTs (dark purple circles) decreases monotonously with increasing silicon molar fraction gradually approaching the band gap value of bulk silicon. For low silicon molar fractions, the band gap of the fully fluorinated systems is narrower than that of the fully hydrogenated structures by up to 0.79 eV. As the silicon molar fraction increases, the difference in band gap of the fluorinated and hydrogenated systems is reduced, such that for molar fractions of ∼0.65 the band gaps are identical to within 0.02 eV. Furthermore, as may be expected, all fully fluorinated SiNTs considered possess a wider band gap than their corresponding SiNWs. This can be attributed to quantum confinement effects. From the inset of Figure 4, it can be clearly deduced that the effect of the appearance of the inner cavity on the band gap of the fully fluorinated systems is smaller than that previously obtained for the hydrogenated systems. The

transition from [111], [100], [112], and [110] F-SiNWs to F-SiNTs results in band gap increases of 24%, 41%, 11%, and 11%, respectively. This is to be compared with the hydrogenated system values of 68%, 61%, 26%, and 17%, respectively.

Upon careful inspection of the results appearing in Figure 4, it can be speculated that by varying the relative surface coverage of hydrogen and fluorine atoms it should be possible to tailor the band gap of SiNWs and SiNTs having a silicon molar fraction lower than 0.65. In the diagram, we highlight the area spanning the region between the fully hydrogenated and fully fluorinated systems band gaps indicating the expected band gap range that can be achieved by manipulating the surface fluorination scheme. To further examine this issue, we study, in Figure 5, the influence of fluorine surface coverage on the band gaps of the [100] and the [112] systems. As mentioned above, from quantum confinement considerations, the band gaps of the SiNTs are consistently larger than those of their corresponding SiNWs. As the fluorine coverage is increased, the band gaps of the SiNTs decrease monotonously, approaching that of the fully fluorinated systems. On the contrary, the band gaps of the SiNWs are much less sensitive to the outer surface fluorine coverage, such that the values calculated for the fully fluorinated and fully hydrogenated systems differ by less than 0.2 eV as is also indicated in Figure 4. This suggests that the inner surface fluorine decoration has a stronger effect on the electronic structure of the systems than the outer surface fluorination.

Interestingly, for the mixed decoration schemes at given fluorine coverage, a strong effect of the exact decoration scheme on the band gap of the system is obtained. We find that, for the 50% and 75% fluorine-covered [100] and for the 75% covered [112] SiNTs, the band gap of part of the randomly chosen decoration arrangements is smaller than that of the corresponding fully fluorinated system. Here, we should note that our calculations are of periodic nature. In realistic experimental conditions, different sections along the system will have varying passivation schemes and thus we expect the band gap of the system at a given fluorine coverage to be averaged.

The results presented in Figure 5 clearly indicate that surface chemistry may be used to tailor the electronic properties of narrow quasi-one-dimensional silicon nanostructures. By careful surface functionalization, we predict that it should be possible to tune the band gap of such systems to range between insulating to wide-band-gap semiconducting even without manipulating the structure of the inner silicon core.
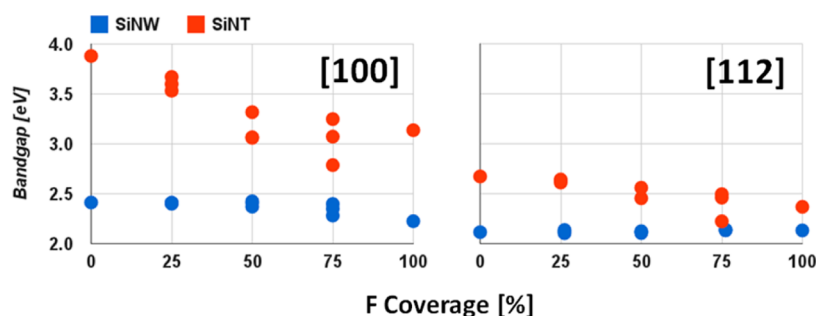

Figure 5. HSE/6-31G** band gaps of the [100] (left panel) and [112] (right panel) SiNWs (blue symbols) and SiNTs (red symbols) as a function of fluorine coverage. For the [112] SiNT with 50% fluorine coverage, only two (instead of three) random decoration schemes have been calculated. Results of all random configurations considered for the mixed structures are presented.
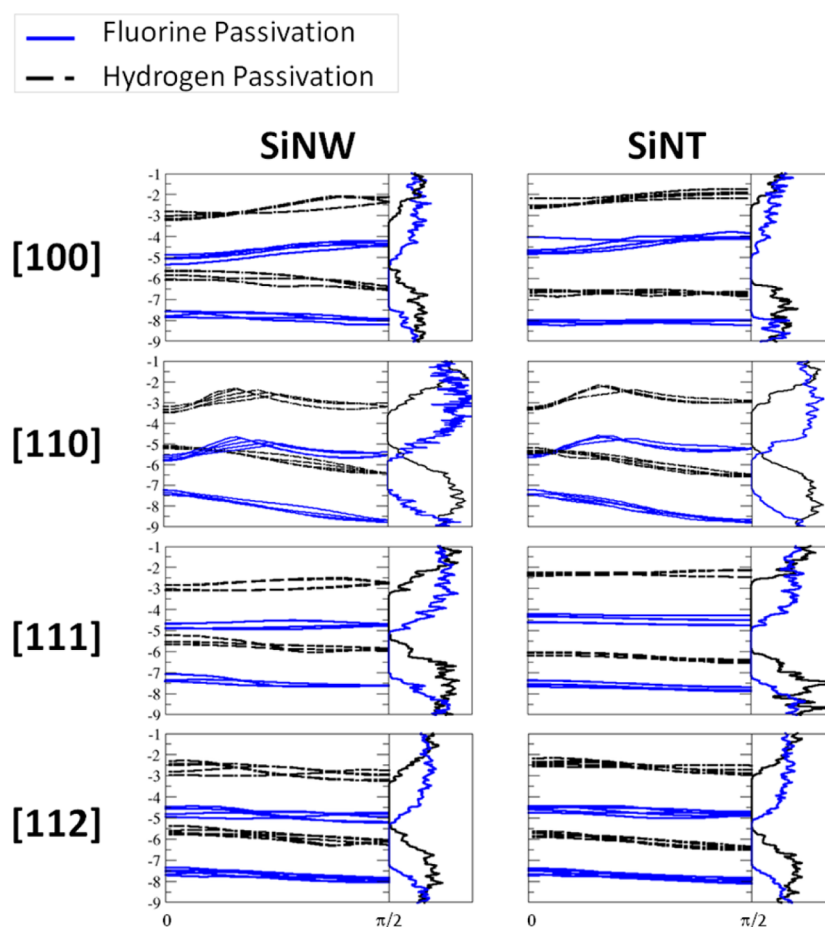
14687

dx.doi.org/10.1021/jp4045786 | J. Phys. Chem. C 2013, 117, 14684–14691

Figure 6. HSE/6-31G** band structures and densities of states of the fully fluorine decorated (full blue lines) SiNWs and SiNTs studied. Results for the fully hydrogenated systems (dashed black lines) are presented for comparison. For clarity, only five occupied and five virtual bands are presented.

To gain further insight regarding the influence of fluorination on the electronic properties of SiNWs and SiNTs, we present, in Figure 6, the band structures and the corresponding densities of states of the fully fluorinated systems and compare them to the results obtained for their fully hydrogenated counterparts. Apart from the fluorination-induced band gap reduction discussed above, a pronounced downshift of both the occupied and unoccupied bands is observed for both the SiNWs and SiNTs regardless of the crystallographic orientation. For the systems considered, the valence band maxima (VBM) down-shifted by up to 2.16 eV and the conduction band minima (CBM) downshifted by up to 2.32 eV. Interestingly, when the VBMs and CBMs of the fully hydrogenated and fluorinated systems are compared, it is found that their dispersion relation is hardly affected upon fluorination and that they are practically rigidly downshifted. The effect of band gap reduction thus results from a different rigid downshift than the VBM and CBM of each system experience. For the same reasons, the nature of the band gap of all but the [111] SiNW systems studied is not affected by fluorination, such that both the fully hydrogenated and fluorinated [100] systems present a direct band gap whereas the [112] systems and the [111] SiNT present an indirect gap. The [111] SiNW exhibits a transition from direct to indirect band gap upon fluorination. For all the fluorinated systems studied, we find that the wires and the tubes exhibit the same band gap character.

■ SUMMARY

In this paper, we presented a computational study of the structural and electronic properties of fluorine-decorated narrow sp^3-type SiNTs and SiNWs bearing a wall thickness of a few atomic layers. Eight SiNT and SiNW models with periodic axes along the [100], [110], [111], and [112] crystallographic orientations were considered. The energetic stability and electronic properties of the various fluorinated systems considered were compared to those of their hydrogen-passivated SiNT and SiNW counterparts. Unlike the fully hydrogenated systems, the relative stability of the fully fluorinated structures was found to increase linearly with decreasing silicon molar fraction. Furthermore, the fully fluorinated systems were found to be consistently more stable than their hydrogenated counterparts. For mixed hydrogenation and fluorination decoration schemes of the [100] and [112] SiNTs and SiNWs, the relative stability was found to vary linearly with the fluorine surface coverage. Interestingly, for fluorine surface coverage exceeding 25%, the tubular structures were found to be more stable than their wire counterparts.

Similar to the case of the fully hydrogenated systems, the band gaps of the fully fluorinated structures were found decrease monotonously with increasing silicon molar fraction. For silicon molar fractions lower than 0.5, the band gap value of the fully fluorinated systems was found to be smaller than that of the fully hydrogenated structures by up to 0.79 eV. These differences reduce as the silicon molar fraction increases. As

may be expected, the fully fluorinated SiNTs bear larger band gaps than their corresponding SiNWs. Nevertheless, the differences between their band gaps are lower than those obtained for the hydrogenated systems. The mixed hydrogenated and fluorinated systems usually present band gaps that reside within the range spanned by the fully hydrogenated and fully fluorinated structures. Some exceptions occur where the band gaps of the mixed decorated systems become lower than the band gaps of their fully fluorinated counterparts. In general, the band gaps of the SiNTs studied are more sensitive to the fluorine surface coverage than those of the corresponding SiNWs. Upon examination of the band structure of the various systems, the reduction of the band gap upon fluorination was found to result from a different and (almost) rigid downshift of the valence and conduction bands in the vicinity of the gap.

Our results indicate that surface functionalization may serve to control the structural stability of narrow quasi-one-dimensional silicon nanostructures and open the way toward chemical tailoring of their electronic properties. We predict that, by careful design of the chemical surface decoration scheme, it should be possible to tune the band gap of such systems to range between insulating and wide-band-gap semiconducting even without manipulating the structure of the inner silicon core.

■ ASSOCIATED CONTENT

Ⓢ Supporting Information

Two figures that evaluate the effect of choice of exchange−correlation density functional approximation on the calculated structural and electronic properties of the systems considered; three tables that evaluate the computational error induced by using small Gaussian basis sets in some geometry optimization procedures; and optimized coordinates of all systems considered (in Excel worksheet format). This material is available free of charge via the Internet at http://pubs.acs.org

■ AUTHOR INFORMATION

Notes

The authors declare no competing financial interest.

■ ACKNOWLEDGMENTS

■ REFERENCES

(1) Cui, Y.; Wei, Q.; Park, H.; Lieber, C. M. Nanowire Nanosensors for Highly Sensitive and Selective Detection of Biological and Chemical Species. *Science* **2001**, *293*, 17.

(2) Hahm, J.-i.; Lieber, C. M. Direct Ultrasensitive Electrical Detection of DNA and DNA Sequence Variations Using Nanowire Nanosensors. *Nano Lett.* **2003**, *4*, 51−54.

(3) Gao, Z.; Agarwal, A.; Trigg, A. D.; Singh, N.; Fang, C.; Tung, C.-H.; Fan, Y.; Buddharaju, K. D.; Kong, J. Silicon Nanowire Arrays for Label-Free Detection of DNA. *Anal. Chem.* **2007**, *79*, 3291−3297.

(4) Patolsky, F.; Zheng, G.; Lieber, C. M. Fabrication of Silicon Nanowire Devices for Ultrasensitive, Label-Free, Real-Time Detection of Biological and Chemical Species. *Nat. Protoc.* **2006**, *1*, 1711−1724.

(5) Cheng, M. M.-C.; Cuda, G.; Bunimovich, Y. L.; Gaspari, M.; Heath, J. R.; Hill, H. D.; Mirkin, C. A.; Nijdam, A. J.; Terracciano, R.; Thundat, T.; et al. Nanotechnologies for Biomolecular Detection and Medical Diagnostics. *Curr. Opin. Chem. Biol.* **2006**, *10*, 11−19.

(6) Engel, Y.; Elnathan, R.; Pevzner, A.; Davidi, G.; Flaxer, E.; Patolsky, F. Supersensitive Detection of Explosives by Silicon Nanowire Arrays. *Angew. Chem., Int. Ed.* **2010**, *49*, 6830−6835.

(7) Kwiat, M.; Patolsky, F. Interfacing Biomolecules, Cells and Tissues with Nanowire-Based Electrical Devices. In *Applications of Electrochemistry and Nanotechnology in Biology and Medicine II*; Eliaz, N., Ed.; Modern Aspects of Electrochemistry, Vol. 53; Springer: New York, 2012; pp 67−104.

(8) Huang, Y.; Duan, X.; Cui, Y.; Lauhon, L. J.; Kim, K.-H.; Lieber, C. M. Logic Gates and Computation from Assembled Nanowire Building Blocks. *Science* **2001**, *294*, 1313−1317.

(9) Cui, Y.; Zhong, Z.; Wang, D.; Wang, W. U.; Lieber, C. M. High Performance Silicon Nanowire Field Effect Transistors. *Nano Lett.* **2003**, *3*, 149−152.

(10) Li, Y.; Qian, F.; Xiang, J.; Lieber, C. M. Nanowire Electronic and Optoelectronic Devices. *Mater. Today* **2006**, *9*, 18−27.

(11) Wong, H. Recent Developments in Silicon Optoelectronic Devices. *Microelectron. Reliab.* **2002**, *42*, 317−326.

(12) Ahn, Y.; Dunning, J.; Park, J. Scanning Photocurrent Imaging and Electronic Band Studies in Silicon Nanowire Field Effect Transistors. *Nano Lett.* **2005**, *5*, 1367−1370.

(13) Peng, K.; Wang, X.; Lee, S.-T. Silicon Nanowire Array Photoelectrochemical Solar Cells. *Appl. Phys. Lett.* **2008**, *92*, No. 163103.

(14) Tian, B.; Kempa, T. J.; Lieber, C. M. Single Nanowire Photovoltaics. *Chem. Soc. Rev.* **2009**, *38*, 16−24.

(15) Kelzenberg, M. D.; Boettcher, S. W.; Petykiewicz, J. A.; Turner-Evans, D. B.; Putnam, M. C.; Warren, E. L.; Spurgeon, J. M.; Briggs, R. M.; Lewis, N. S.; Atwater, H. A. Enhanced Absorption and Carrier Collection in Si Wire Arrays for Photovoltaic Applications. *Nat. Mater.* **2010**, *9*, 239−244.

(16) Hochbaum, A. I.; Yang, P. Semiconductor Nanowires for Energy Conversion. *Chem. Rev.* **2009**, *110*, 527−546.

(17) Zhang, R. Q.; Liu, X. M.; Wen, Z.; Jiang, Q. Prediction of Silicon Nanowires as Photocatalysts for Water Splitting: Band Structures Calculated Using Density Functional Theory. *J. Phys. Chem. C* **2011**, *115*, 3425−3428.

(18) Ma, D. D. D.; Lee, C. S.; Au, F. C. K.; Tong, S. Y.; Lee, S. T. Small-Diameter Silicon Nanowire Surfaces. *Science* **2003**, *299*, 1874.

(19) Delley, B.; Steigmeier, E. F. Size Dependence of Band Gaps in Silicon Nanostructures. *Appl. Phys. Lett.* **1995**, *67*, 2370.

(20) Zhao, X.; M.Wei, C.; Yang, L.; Chou, M. Y. Quantum Confinement and Electronic Properties of Silicon Nanowires. *Phys. Rev. Lett.* **2004**, *92*, 23.

(21) Ponomareva, I.; Menon, M.; Srivastava, D.; Andriotis, A. N. Structure, Stability, and Quantum Conductivity of Small Diameter Silicon Nanowires. *Phys. Rev. Lett.* **2005**, *95*, 265502.

(22) Horiguchi, S. Validity of Effective Mass Theory for Energy Levels in Si Quantum Wires. *Phys. B: Condens. Matter* **1996**, *227*, 336−338.

(23) Singh, A. K.; Kumar, V.; Note, R.; Kawazoe, Y. Effects of Morphology and Doping on the Electronic and Structural Properties of Hydrogenated Silicon Nanowires. *Nano Lett.* **2006**, *6*, 920−925.

(24) Yeh, C.-Y.; Zhang, S. B.; Zunger, A. Confinement, Surface, and Chemisorption Effects on the Optical Properties of Si Quantum Wires. *Phys. Rev. B* **1994**, *50*, 14405−14415.

(25) Xi-Meng, G.; Zhi-Ping, Y. Supercell Approach in Tight-Binding Calculation of Si and Ge Nanowire Bandstructures. *Chin. Phys. Lett.* **2005**, *22*, 2651.

(26) Vo, T.; Williamson, A. J.; Galli, G. First Principle Simulation of the Structural and Electronic Properties of Silicon Nanowires. *Phys. Rev. B* **2006**, *74*, No. 045116.

(27) Aradi, B.; Ramos, L. E.; Deák, P.; Köhler, T.; Bechstedt, F.; Zhang, R. Q.; Frauenheim, T. Theoretical Study of the Chemical Gap Tuning in Silicon Nanowires. *Phys. Rev. B* **2007**, *76*, 35305.

(28) Zhu, Z.; Zhang, A.; Ouyang, G.; Yang, G. Edge Effect on Band Gap Shift in Si Nanowires with Polygonal Cross-Sections. *Appl. Phys. Lett.* **2011**, *98*, 263112.

(29) Hmiel, A.; Xue, Y. Shape-Tunable Electronic Properties of Monohydride and Trihydride [112]-Oriented Si Nanowires. *Phys. Rev. B* **2009**, *80*, No. 241410.

(30) Nolan, M.; O'Callaghan, S.; Fagas, G.; Greer, J. C.; Frauenheim, T. Silicon Nanowire Band Gap Modification. *Nano Lett.* **2006**, *7*, 34−38.

(31) Leu, P. W.; Shan, B.; Cho, K. Surface Chemical Control of the Electronic Structure of Silicon Nanowires: Density Functional Calculations. *Phys. Rev. B* **2006**, *73*, No. 195320.

(32) Cui, Y.; Lauhon, L. J.; Gudiksen, M. S.; Wang, J.; Lieber, C. M. Diameter-Controlled Synthesis of Single-Crystal Silicon Nanowires. *Appl. Phys. Lett.* **2001**, *78*, 2214−2216.

(33) Haick, H.; Hurley, P. T.; Hochbaum, A. I.; Yang, P.; Lewis, N. S. Electrical Characteristics and Chemical Stability of Non-Oxidized, Methyl-Terminated Silicon Nanowires. *J. Am. Chem. Soc.* **2006**, *128*, 8990−8991.

(34) Durgun, E.; Akman, N.; Ataca, C.; Ciraci, S. Atomic and Electronic Structures of Doped Silicon Nanowires: A First-Principles Study. *Phys. Rev. B* **2007**, *76*, No. 245323.

(35) Hong, K.-H.; Kim, J.; Lee, S.-H.; Shin, J. K. Strain-Driven Electronic Band Structure Modulation of Si Nanowires. *Nano Lett.* **2008**, *8*, 1335−1340.

(36) Ghosh, R. K.; Bhattacharya, S.; Mahapatra, S. Physics-Based Band Gap Model for Relaxed and Strained [100] Silicon Nanowires. *IEEE Trans. Electron Devices* **2012**, *59*, 6.

(37) Leu, P. W.; Svizhenko, A.; Cho, K. Ab Initio Calculations of the Mechanical and Electronic Properties of Strained Si Nanowires. *Phys. Rev. B* **2008**, *77*, No. 235305.

(38) Zhang, Y. F.; Tang, Y. H.; Wang, N.; Yu, D. P.; Lee, C. S.; Bello, I.; Lee, S. T. Silicon Nanowires Prepared by Laser Ablation at High Temperature. *Appl. Phys. Lett.* **1998**, *72*, 1835−1837.

(39) Morales, A. M.; Lieber, C. M. A Laser Ablation Method for the Synthesis of Crystalline Semiconductor Nanowires. *Science* **1998**, *279*, 208−211.

(40) Irrera, A.; Pecora, E. F.; Priolo, F. Control of Growth Mechanisms and Orientation in Epitaxial Si Nanowires Grown by Electron Beam Evaporation. *Nanotechnology* **2009**, *20*, No. 135601.

(41) Ross, F. M.; Tersoff, J.; Reuter, M. C. Sawtooth Faceting in Silicon Nanowires. *Phys. Rev. Lett.* **2005**, *95*, No. 146104.

(42) Wu, Y.; Cui, Y.; Huynh, L.; Barrelet, C. J.; Bell, D. C.; Lieber, C. M. Controlled Growth and Structures of Molecular-Scale Silicon Nanowires. *Nano Lett.* **2004**, *4*, 433−436.

(43) Barnard, A. S.; Russo, S. P. Structure and Energetics of Single-Walled Armchair and Zigzag Silicon Nanotubes. *J. Phys. Chem.* **2003**, *107*, 7577−7581.

(44) Wang, N.; Tang, Y. H.; Zhang, Y. F.; Lee, C. S.; Bello, I.; Lee, S. T. Si Nanowires Grown from Silicon Oxide. *Chem. Phys. Lett.* **1999**, *299*, 237−242.

(45) Golea, J. L.; Stout, J. D.; Rauch, W. L.; Wangb, Z. L. Direct Synthesis of Silicon Nanowires, Silica Nanospheres, and Wire-Like Nanosphere Agglomerates. *Appl. Phys. Lett.* **2000**, *76*, 2346.

(46) Holmes, J. D.; Johnston, K. P.; Doty, R. C.; Korgel, B. A. Control of Thickness and Orientation of Solution-Grown Silicon Nanowires. *Science* **2000**, *287*, 1471−1473.

(47) Liu, H. I.; Biegelsen, D. K.; Ponce, F. A.; Johnson, N. M.; Pease, R. F. W. Self-Limiting Oxidation for Fabricating Sub-5 nm Silicon Nanowires. *Appl. Phys. Lett.* **1994**, *64*, 1383−1385.

(48) Hofmann, S.; Ducati, C.; Neill, R. J.; Piscanec, S.; Ferrari, A. C.; Geng, J.; Dunin-Borkowski, R. E.; Robertson, J. Gold Catalyzed Growth of Silicon Nanowires by Plasma Enhanced Chemical Vapor Deposition. *J. Appl. Phys.* **2003**, *94*, 6005−6012.

(49) Zhang, Y. F.; Tang, Y. H.; Wang, N.; Lee, C. S.; Bello, I.; Lee, S. T. One-Dimensional Growth Mechanism of Crystalline Silicon Nanowires. *J. Cryst. Growth* **1999**, *197*, 136−140.

(50) Yu, D. P.; Bai, Z. G.; Ding, Y.; Hang, Q. L.; Zhang, H. Z.; Wang, J. J.; Zou, Y. H.; Qian, W.; Xiong, G. C.; Zhou, H. T.; et al. Nanoscale Silicon Wires Synthesized Using Simple Physical Evaporation. *Appl. Phys. Lett.* **1998**, *72*, 3458−3460.

(51) Wang, N.; Tang, Y. H.; Zhang, Y. F.; Lee, C. S.; Lee, S. T. Nucleation and Growth of Si Nanowires from Silicon Oxide. *Phys. Rev. B* **1998**, *58*, R16024−R16026.

(52) Teo, B. K.; Li, C. P.; Sun, X. H.; Wong, N. B.; Lee, S. T. Silicon−Silica Nanowires, Nanotubes, and Biaxial Nanowires: Inside, Outside, and Side-by-Side Growth of Silicon versus Silica on Zeolite. *Inorg. Chem.* **2003**, *42*, 6723−6728.

(53) Bondi, R. J.; Lee, S.; Hwang, G. S. First-Principles Study of the Structural, Electronic, and Optical Properties of Oxide-Sheathed Silicon Nanowires. *ACS Nano* **2011**, *5*, 1713−1723.

(54) Koleini, M.; Colombi Ciacchi, L.; Fernández-Serra, M. V. Electronic Transport in Natively Oxidized Silicon Nanowires. *ACS Nano* **2011**, *5*, 2839−2846.

(55) Trucks, G. W.; Raghavachari, K.; Higashi, G. S.; Chabal, Y. J. Mechanism of HF Etching of Silicon Surfaces: A Theoretical Understanding of Hydrogen Passivation. *Phys. Rev. Lett.* **1990**, *65*, 504−507.

(56) Zhang, R. Q.; Lifshitz, Y.; Ma, D. D. D.; Zhao, Y. L.; Frauenheim, T.; Lee, S. T.; Tong, S. Y. Structures and Energetics of Hydrogen-Terminated Silicon Nanowire Surfaces. *J. Chem. Phys.* **2005**, *123*, No. 144703.

(57) Read, A. J.; Needs, R. J.; Nash, K. J.; Canham, L. T.; Calcott, P. D. J.; Qteish, A. First-Principles Calculations of the Electronic Properties of Silicon Quantum Wires. *Phys. Rev. Lett.* **1992**, *69*, 1232−1235.

(58) Matsuda, Y.; Tahir-Kheli, J.; Goddard, W. A. Surface and Electronic Properties of Hydrogen Terminated Si [001] Nanowires. *J. Phys. Chem. C* **2011**, *115*, 12586−12591.

(59) Lu, A. J.; Zhang, R. Q.; Lee, S. T. Unique Electronic Band Structures of Hydrogen-Terminated <112> Silicon Nanowires. *Nanotechnology* **2008**, *19*, No. 035708.

(60) Guo, C.-S.; Luo, L.-B.; Yuan, G.-D.; Yang, X.-B.; Zhang, R.-Q.; Zhang, W.-J.; Lee, S.-T. Surface Passivation and Transfer Doping of Silicon Nanowires. *Angew. Chem.* **2009**, *121*, 10080−10084.

(61) Ng, M.-F.; Zhou, L.; Yang, S.-W.; Sim, L. Y.; Tan, V. B. C.; Wu, P. Theoretical Investigation of Silicon Nanowires: Methodology, Geometry, Surface Modification, and Electrical Conductivity Using a Multiscale Approach. *Phys. Rev. B* **2007**, *76*, No. 155435.

(62) It should be noted that halogenated silicon surfaces are often regarded as highly reactive and therefore should be treated under inert conditions.[63] Specifically, plasma etching of silicon surfaces with molecular fluorine was shown to result in SiF_2 terminating groups, whereas high exposure to atomic fluorine induced tetrafluorosilane desorption from the surface.[64−70]

(63) Buriak, J. M. Organometallic Chemistry on Silicon and Germanium Surfaces. *Chem. Rev.* **2002**, *102*, 1271−1308.

(64) Mucha, J. A.; Donnelly, V. M.; Flamm, D. L.; Webb, L. M. Chemiluminescence and the Reaction of Molecular Fluorine with Silicon. *J. Phys. Chem.* **1981**, *85*, 3529−3532.

(65) Stinespring, C. D.; Freedman, A. Studies of Atomic and Molecular Fluorine Reactions on Silicon Surfaces. *Appl. Phys. Lett.* **1986**, *48*, 718−720.

(66) Nakamura, M.; Takahagi, T.; Ishitani, A. Fluorine Termination of Silicon Surface by F_2 and Succeeding Reaction with Water. *Jpn. J. Appl. Phys.* **1993**, *32*, 3125−3130.

(67) Tu, Y.-Y.; Chuang, T. J.; Winters, H. F. Chemical Sputtering of Fluorinated Silicon. *Phys. Rev. B* **1981**, *23*, 823−835.

(68) Wu, C. J.; Carter, E. A. Structures and Adsorption Energetics for Chemisorbed Fluorine Atoms on Si(100)-2 × 1. *Phys. Rev. B* **1992**, *45*, 9065−9081.

(69) Aliev, V. S.; Kruchinin, V. N.; Baklanov, M. R. Adsorption of Molecular Fluorine on the Si(100) Surface: an Ellipsometric Study. *Surf. Sci.* **1996**, *347*, 97−104.

(70) McFeely, F.; Morar, J.; Himpsel, F. Soft X-ray Photoemission Study of the Silicon-Fluorine Etching Reaction. *Surf. Sci.* **1986**, *165*, 277−287.

(71) Hever, A.; Bernstein, J.; Hod, O. Structural Stability and Electronic Properties of sp3 type Silicon Nanotubes. *J. Chem. Phys.* **2012**, *137*, No. 214702.

(72) Schmidt, O. G.; Eberl, K. Nanotechnology: Thin Solid Films Roll Up Into Nanotubes. *Nature* **2001**, *410*, 168−168.

(73) Jeong, S. Y.; Kim, J. Y.; Yang, H. D.; Yoon, B. N.; Choi, S. H.; Kang, H. K.; Yang, C. W.; Lee, Y. H. Synthesis of Silicon Nanotubes on Porous Alumina Using Molecular Beam Epitaxy. *Adv. Mater.* **2003**, *15*, 1172−1176.

(74) Chen, Y. W.; Tang, Y. H.; Pei, L. Z.; Guo, C. Self-Assembled Silicon Nanotubes Grown from Silicon Monoxide. *Adv. Mater.* **2005**, *17*, 564−567.

(75) Crescenzi, M. D.; Castrucci, P.; Scarselli, M.; Diociaiuti, M.; Chaudhari, P. S.; Balasubramanian, C.; Bhave, T. M.; Bhoraskar, S. V. Experimental Imaging of Silicon Nanotubes. *Appl. Phys. Lett.* **2005**, *86*, No. 231901.

(76) Ben-Ishai, M.; Patolsky, F. Shape- and Dimension-Controlled Single-Crystalline Silicon and SiGe Nanotubes. *J. Am. Chem. Soc.* **2009**, *131*, 3679−3689.

(77) Ben-Ishai, M.; Patolsky, F. Wall-Selective Chemical Alteration of Silicon Nanotube Molecular Carriers. *J. Am. Chem. Soc.* **2011**, *133*, 1545−1552.

(78) Quitoriano, N. J.; Belov, M.; Evoy, S.; Kamins, T. I. Si Single-Crystal Nanotubes, and Their Mechanical Resonant Properties. *Nano Lett.* **2009**, *9*, 1511−1516.

(79) Frisch, M. J.; Trucks, G. W.; Schlegel, H. B.; Scuseria, G. E.; Robb, M. A.; Cheeseman, J. R.; Montgomery, J. A., Jr.; Vreven, T.; Kudin, K. N.; et al. Gaussian Development Version (Revision F.1); Gaussian Inc., Wallingford, CT, 2008.

(80) *The Self-Consistent Field for Molecules and Solids*; Slater, J. C., Ed.; Quantum Theory of Molecules and Solids, Vol. 4; McGraw-Hill: New York, 1974; p 57.

(81) Vosko, S. H.; Wilk, L.; Nusair, M. Accurate Spin-Dependent Electron Liquid Correlation Energies for Local Spin Density Calculations: A Critical Analysis. *Can. J. Phys.* **1980**, *58*, 1200−1211.

(82) Perdew, J. P.; Burke, K.; Ernzerhof, M. Generalized Gradient Approximation Made Simple. *Phys. Rev. Lett.* **1996**, *77*, 3865−3868.

(83) Heyd, J.; Scuseria, G. E. Assessment and Validation of a Screened Coulomb Hybrid Density Functional. *J. Chem. Phys.* **2004**, *120*, 7274−7280.

(84) Heyd, J.; Scuseria, G. E. Efficient Hybrid Density Functional Calculations in Solids: Assessment of the Heyd−Scuseria−Ernzerhof Screened Coulomb Hybrid Functional. *J. Chem. Phys.* **2004**, *121*, 1187−1192.

(85) (a) Heyd, J.; Scuseria, G. E.; Ernzerhof, M. Hybrid Functionals Based on a Screened Coulomb Potential. *J. Chem. Phys.* **2003**, *118*, 8207−8215. (b) Heyd, J.; Scuseria, G. E.; Ernzerhof, M. Erratum: "Hybrid functionals based on a screened Coulomb potential" [J. Chem. Phys. 118, 8207 (2003)]. *J. Chem. Phys.* **2006**, *124*, No. 219906.

(86) Heyd, J.; Peralta, J. E.; Scuseria, G. E.; Martin, R. L. Energy Band Gaps and Lattice Parameters Evaluated with the Heyd−Scuseria−Ernzerhof Screened Hybrid Functional. *J. Chem. Phys.* **2005**, *123*, No. 174101.

(87) Barone, V.; Hod, O.; Peralta, J. E.; Scuseria, G. E. Accurate Prediction of the Electronic Properties of Low-Dimensional Graphene Derivatives Using a Screened Hybrid Density Functional. *Acc. Chem. Res.* **2011**, *44*, 269−279.

(88) Hariharan, P. C.; Pople, J. A. The Influence of Polarization Functions on Molecular Orbital Hydrogenation Energies. *Theor. Chim. Acta* **1973**, *28*, 213.

(89) Hod, O.; Barone, V.; Peralta, J. E.; Scuseria, G. E. Enhanced Half-Metallicity in Edge-Oxidized Zigzag Graphene Nanoribbons. *Nano Lett.* **2007**, *7*, 2295−2299.

(90) Walsh, R. Bond Dissociation Energy Values in Silicon-Containing Compounds and Some of their Implications. *Acc. Chem. Res.* **1981**, *14*, 246−252.